Astronomy & Astrophysics manuscript no. Irregular-occ
November 14, 2015

Stellar occultation predictions for 9 irregular satellites of giant planets and Triton for 2015-2017

A. R. Gomes-Júnior[1], M. Assafin[1,⋆], L. Beauvalet[2], R. Vieira-Martins[1,2,3,⋆⋆], J. I. B. Camargo[2,3], B. E. Morgado[1,2]

[1] Observatório do Valongo/UFRJ, Ladeira Pedro Antônio 43, CEP 20.080-090 Rio de Janeiro - RJ, Brazil
e-mail: altair08@astro.ufrj.br
[2] Observatório Nacional/MCT, R. General José Cristino 77, CEP 20921-400 Rio de Janeiro - RJ, Brazil
e-mail: rvm@on.br
[3] Laboratório Interinstitucional de e-Astronomia - LIneA, Rua Gal. José Cristino 77, Rio de Janeiro, RJ 20921-400, Brazil
[4] Federal University of Technology - Paraná (UTFPR / DAFIS), Rua Sete de Setembro, 3165, CEP 80230-901, Curitiba, PR, Brazil

Received ; accepted

ABSTRACT

Context. Due to their orbital configurations, it is common belief that the irregular satellites were probably captured by the giant planets in the early solar system. It is important to know their physical parameters, such as size and albedo, to trace back their true origin. The best ground-based technique to obtain such parameters is the observation of stellar occultations by these objects.
Aims. We aimed to predict stellar occultations for the seven biggest irregular satellites of Jupiter: Himalia, Elara, Pasiphae, Carme, Lysithea, Sinope and Ananke; for the irregular satellite of Saturn: Phoebe; and the satellites of Neptune: Nereid and Triton.
Methods. We identified candidates to stellar occultations by the irregular satellites from the UCAC4 catalogue and from a catalogue of stars in the sky-path of Neptune obtained from observations made with the ESO2p2/WFI (2.2 m Max-Planck ESO telescope with the Wide Field Imager) instrument. These catalogues were crossed with the ephemeris of the satellites to identify stellar occultations. The ephemeris were generated by a numerical integration (Here we may write something about after the work of Laurène) that used the positions obtained by Gomes-Júnior et al. (2015) to improve the predictions.
Results. We managed to obtain 588 candidates of stellar occultations between the period of January, 2015 and December, 2017. We made observational tests for the predictions of the events of Himalia in March 03, 2015 and Elara in March 30, 2015. The observations were made in the same field to minimize errors and the obtained relative satellite-star positions were used to evaluate the predictions.
Conclusions. The comparisons between the predictions and the observation tests show a good agreement. We discuss how the successful observation of a stellar occultation by these objects is quite possible.

Key words. Occultations - Planets and satellites: general - Planets and satellites: individual: Jovian and Saturnian irregular satellites

1. Introduction

Irregular (outer) satellites revolve around giant planets at large distances in eccentric, highly inclined and frequently retrograde orbits. Because of these peculiar orbits, it is largely accepted that these objects were not originated with, but were captured by their planets in the early solar system (Sheppard 2005).

There is a number of capture mechanisms of objects by giant planets proposed in the literature. There is the Gas Drag in the primordial circumplanetary nebulae (Sheppard 2005) where the object would be affected by the gas drag and its velocity slowed down until it be captured by the planet. Another mechanism is called pull-down capture (Sheppard 2005), where the mass of the planet would increase while the object was temporarily captured.

A mechanism based in the Nice model (Morbidelli et al. 2005; Tsiganis et al. 2005; Gomes et al. 2005) was proposed by Nesvorný et al. (2007) and, in the specific case of Jupiter with the modern Nice model, by Nesvorný et al. 2014. During the early solar system instability, encounters between the outer planets occurred. These planetary encounters could exchange energy and angular momentum between planets and the objects nearby making it possible for the capture of irregular bodies by the giant planets. In this scenario, the survival rate of prior-LHB (Late Heavy Bombardment) satellites is very small.

Another important mechanism is the capture through collisional interactions (Sheppard 2005). A collision between two small bodies in the Hill's sphere of the planet could generate fragmented objects and the dissipated energy could be such that some of these objects could be captured.

Some of these objects are in dynamical groups with similar orbital elements, called families, similar to families found in the Main Asteroid Belt. These families may have been created by a parent body disrupted by collisions with comets or other satellites (Nesvorný et al. 2004). Collisions with comets are more likely to have occurred during the LHB (Gomes et al. 2005).

Nesvorný et al. (2003) studied the collision rates between irregular satellites and concluded that some satellites could have been removed by collision with a bigger satellite. The collision rate between satellites of the Himalia Group (Himalia, Elara, Lysithea and Leda, mainly), for instance, was found to be more than one during the solar system age suggesting that their current structure was originated by satellite-satellite collision.

For Phoebe, ejected material from its surface caused by impacts could evolve due to Poynting-Robertson drag and collide

Send offprint requests to: A. R. Gomes-Júnior
⋆ Affiliated researcher at Observatoire de Paris/IMCCE, 77 Avenue Denfert Rochereau 75014 Paris, France
⋆⋆ Affiliated researcher at Observatoire de Paris/IMCCE, 77 Avenue Denfert Rochereau 75014 Paris, France

Table 1. Estimated diameter of the satellites and correspondent apparent diameter

Satellite	Diameter of the satellites km	mas[a]	References
Ananke	29	8	1
Carme	46	13	1
Elara	86	24	1
Himalia	$(150 \times 120) \pm 20^b$	41	2
Lysithea	36	10	1
Pasiphae	62	17	1
Sinope	37	10	1
Phoebe	212 ± 1.4^b	32	3
Nereid	340 ± 50^c	15	4
Triton	2707 ± 2.0^c	124	5

References. (1) Rettig et al. (2001); (2) Porco et al. (2003); (3) Thomas (2010); (4) Thomas et al. (1991); (5) Thomas (2000).
[(a)] Using a mean distance from Jupiter of 5 AU, from Saturn of 9 AU and from Neptune of 30 AU. [(b)] From Cassini observation. [(c)] From Voyager-2 observation.

with Iapetus causing the large variation in albedo observed on it (Nesvorný et al. 2003). Indeed, Cassini was able to detected in Phoebe an absorption feature at 2.42 μm (probably CN combinations) that was also detected in the dark side of Iapetus (Clark et al. 2005).

The region of origin of these object is not well known. Grav et al. (2003) and Grav & Bauer (2007) showed that the irregular satellites from the giant planets have their colors and spectral slopes similar to C-, D- and P-type asteroids, Centaurs and trans-neptunian objects (TNOs) suggesting that they have been originated from different locations in the early solar system.

In order to obtain precise fundamental physical parameters like size, shape and albedo for the irregular satellites and thus to contribute to the study of their origin, we will make use of stellar occultations, which provide more accurate results than other ground-based techniques (Sicardy et al. 2011; Ortiz et al. 2012; Braga-Ribas et al. 2014).

No observation of a stellar occultation by an irregular satellite was published up to date. Since their estimated sizes are very small (see Table 1), this may have prevented earlier tries. But, in fact, given their distances to us, current ephemeris and star positions are already good enough for the prediction of the exact location and instant where the shadow of the occultation will cross the Earth. For instance, Himalia, supposedly the largest irregular satellite of Jupiter has an estimated size of 150 km (Porco et al. 2003), which is equivalent to an apparent size of about 40 mas (milliarcseconds).Thus, in this case, the overall budget of ephemeris and star position errors must be around 40 mas in order that we get good chances of observing a stellar occultation, which is quite feasible today.

Unlike stellar occultations by TNOs, which nevertheless have been proved effective, the observation of an occultation by a irregular satellite is, in principle, more favorable. The orbits of their host planets are well known and these satellites have been observed completing already many orbital periods around them, thus presenting better ephemeris than TNOs. Moreover, the irregular satellites are closer to Earth which means a minor location error in kilometers.

Gomes-Júnior et al. (2015) obtained 6523 suitable positions for 18 irregular satellites between 1992 and 2014 with an estimated error in the positions of about 60 to 80 mas. For some satellites the number of positions obtained is comparable to the number used in the numerical integration of orbits by the JPL (Jacobson et al. 2012). They pointed out that the ephemeris of the irregular satellites have systematic errors that may reach 200 mas for some satellites. For an object at the distance of Jupiter, this represents an error bigger than 700 km in the shadow path. Using the positions obtained by Gomes-Júnior et al. (2015) it is possible to improve the ephemeris and better predict stellar occultations for these objects.

We present in this paper stellar occultation predictions for the 7 major irregular satellites of Jupiter (Himalia, Elara, Pasiphae, Lysithea, Carme, Ananke and Sinope), Phoebe from Saturn and Nereid and Triton from Neptune. In the section 2 we explore the scientific rationale for the study of the irregular satellites and the possibility of having a common origin with TNOs. In section 3 we show the numerical integration to improve the ephemeris. In section 4, we present the predictions of the stellar occultations by irregular satellites and how they were made. Some tests made to confirm the predictions are presented in section 5 and the conclusions are given in section 6.

2. Scientific Rationale

There is no consensus for a single model explaining where the irregular satellites were formed. Ćuk & Burns (2004) showed that the progenitor of the Himalia group may have originated in heliocentric orbits similar to the Hilda asteroid group. Sheppard (2005) stated that the irregular satellites may be some of the objects that were formed within the giant planets region.

Phoebe is the most studied irregular satellite. Clark et al. (2005) suggest that its surface is probably covered by material of cometary origin. It was also stated by Johnson & Lunine (2005) that if the porosity of Phoebe would be of about 15%, which the authors believe it is possible, Phoebe would have an uncompressed density similar to those of Pluto and Triton.

Sheppard (2005) and Jewitt & Haghighipour (2007) also expose the possibility for the irregular satellites having their origin as comets or similar to the TNOs. TNOs are highly interesting objects that due to their large heliocentric distances (low temperatures) may be highly preserved having their physical properties similar to those they had when they were formed, then providing history and evolution of the outer solar system (Camargo et al. 2014). This is even more true for the smaller objects, since in principle larger sizes favour physical differentiation processes in the body and vice-versa. However, due to the distance, the smaller TNOs from this region are more difficult to observe. A clever way to overcome this difficulty is to study the much closer irregular satellites, under the hypothesis that they share a common origin with the small TNOs' population.

Triton is a special satellite. Its orbit is retrograde and inclined, but quasi-circular and very close to the planet compared to the irregular ones. Because Triton's orbit size is very small and its precession is not dominated by Solar perturbations, Triton is frequently excluded from the irregular satellites' class, but studied together by many authors (Sheppard 2005; Jewitt & Haghighipour 2007).

Similarly to the irregular satellites, Triton was probably captured in the early solar system and may have a similar origin as the TNOs (Agnor & Hamilton 2006). Differently, Triton is bigger than the irregular satellites by an order of magnitude and has an atmosphere. The main motivation here to study Triton by stellar occultations is to understand the evolution of its atmosphere due to Triton's complicated and extreme seasonal cycle (McKinnon & Kirk 2007).

3. Correction of the ephemeris

3.1. Description of the model

Our numerical model describes the dynamical evolution of the irregular satellites of Jupiter in a jovicentric reference frame. The satellites are submitted to the influence of the Sun and the rest of the solar system, as well as those of the Galilean satellites and the first harmonics of Jupiter's gravity field. The axis of the reference frame are those of the equatorial reference frame J2000.

We use the following notations:

- i and l one of the irregular satellites of Jupiter
- J Jupiter
- j another body of the Solar System
- M_j the mass of the j body, not an irregular satellite
- m_i the mass of the irregular satellite i
- $\boldsymbol{r_i}$ the position of the i body with respect to the barycentre of Jupiter System
- r_{ij} the distance between bodies i and j
- R_J the radius of Jupiter
- J_n the dynamic polar oblateness of the nth order for Jupiter's gravity field
- $U_{\bar{l}\hat{J}}$ potential generated by the oblateness of Jupiter on the satellite l
- Φ_i is the inclination of the i satellite with respect to Jupiter's equator.

For an irregular satellite i, under the gravitational influence of Jupiter, the $\mathcal{N}' - 1$ other irregular satellites, the regular Jovian satellites and the rest of the Solar System ($\mathcal{N}$ bodies), the equation of motion is:

$$\begin{aligned}\ddot{\boldsymbol{r}}_{\boldsymbol{i}} = & -GM_J\frac{\boldsymbol{r_J}-\boldsymbol{r_i}}{r_{iJ}^3} - \sum_{l=1,l\neq i}^{\mathcal{N}'} Gm_l\frac{\boldsymbol{r_l}-\boldsymbol{r_i}}{r_{il}^3} \\ & -\sum_{j=1}^{\mathcal{N}} GM_j\left(\frac{\boldsymbol{r_j}-\boldsymbol{r_i}}{r_{ij}^3} - \underbrace{\frac{\boldsymbol{r_j}-\boldsymbol{r_J}}{r_{Jj}^3}}_{\texttt{undirectperturbations}}\right) \\ & +GM_J\nabla U_{\bar{l}\hat{J}} - \underbrace{\sum_{l=1}^{\mathcal{N}} Gm_l\nabla U_{\bar{l}\hat{J}}}_{\texttt{undirectperturbations}}\end{aligned} \quad (1)$$

where the oblateness potential seen by the body i because of Jupiter is:

$$\begin{aligned}U_{\bar{l}\hat{J}} = & -\frac{R_J^2 J_2}{r_{iJ}^3}\left(\frac{3}{2}\sin^2\Phi_i - \frac{1}{2}\right) \\ & -\frac{R_J^4 J_4}{r_{iJ}^5}\left(\frac{35}{8}\sin^4\Phi_i - \frac{15}{4}\sin^2\Phi_i + \frac{3}{8}\right) \\ & -\frac{R_J^6 J_6}{r_{iJ}^7}\left(\frac{231}{16}\sin^6\Phi_i - \frac{315}{16}\sin^4\Phi_i + \frac{105}{16}\sin^2\Phi_i - \frac{5}{16}\right)\end{aligned} \quad (2)$$

The expressions of $\nabla_l U_{\bar{i}\hat{i}}$ and $\nabla_i U_{\bar{i}\hat{l}}$. have been developed in Lainey et al. (2004).The equations of motion are integrated with the numerical integrator RADAU (Everhart 1985). Our model was fitted to the observations through a least-squares procedure. The satellites were integrated one dynamical family at a time, to gain computing time, while losing minimum precision. Indeed, the interactions between satellites not belonging to the same dynamical family are negligible considering the short timespan of our integration.

The initial osculating elements at the origin of integration are presented in Table 2, while the residuals are presented in Fig **??** to **??**.

All the orbits determined for the satellites show satisfying residuals. Yet, one of the satellites has a peculiar situation. Its small number of observations in our set means that its orbit is definitely loosely constrained. The residuals are lower than those obtained with JPL ephemeris, but the accuracy of an ephemeris decreases when we get further from the time of observations. The main risk of divergence over time comes from the possible absence of long-term effects when fitting to a short timespan of observations. If that were the case, our ephemeris would diverge too quickly to be of any use. JPL ephemerides are fitted over all the available observations. As a result, they will diverge less quickly than our own. Though they are no longer precise enough for our use, they remain a recious reference to identify whether our own model presents a quick divergence. We compared our ephemeris to the JPL for all the Jupiter satellites we fitted, until 2017. The divergence between 2015 and 2018 is at most *insert value here* for *insert right satellite name here*. A example of this difference for satellites Himalia and *whichever satellite you want, if you want)* is presented in Figure **??**.

The obtained ephemeris is hereafter refered as STE, for special-tailored ephemeris.

Here we write something about the numerical integration

4. Prediction of occultations

The prediction of the occultations was made by crossing the stellar coordinates and proper motions of the UCAC4 catalogue (Zacharias et al. 2013) with the corrected JPL ephemeris as presented in section 3. The search for stellar candidates follows the same procedure as presented by Assafin et al. (2010, 2012) and Camargo et al. (2014).

We predicted occultation for the 7 major irregular satellites of Jupiter: Ananke, Carme, Elara, Himalia, Lysithea, Pasiphae, and Sinope; Phoebe of Saturn and Triton and Nereid of Neptune.

For Triton and Nereid, the candidates for stellar occultations in 2015 and 2016 was searched using the WFI catalogue in the same way as the predictions for Centaurs and TNOs occultations by Assafin et al. (2010, 2012) and Camargo et al. (2014). This catalogue contains the stars in the path of Neptune in the sky up to mid-2016. The catalogue was generated by observations made at the ESO 2p2 telescope (IAU code 809) using the Wide Field Imager (WFI) CCD mosaic detector. The filter used was the broad-band R filter ESO#844 with λ_c = 651.725 nm and $\Delta\lambda$ = 162.184 nm.

A total of 588 events (Not counting Triton's event yet) were identified between January 2015 and December 2017. Table 3 exemplifies the catalogue of occultations generated and their parameters, which are necessary to produce occultation maps (see Fig. 2 as an example). Since these objects are very small, the duration of each event is a few seconds.

The ESA astrometry satellite GAIA (de Bruijne 2012) catalogue is expected to be released in the end of 2016. The precise star positions to be derived by GAIA will render better predictions with the only source of error being the ephemeris. The work of Gomes-Júnior et al. (2015) will be revised with the GAIA catalogue and the predictions from 2017 onwards will be better.

Table 2. Initial osculating elements for Jupiter irregular satellites at JD 2451545.0. For Themisto's case, the small number of observations meant that the statistical uncertainty was even greater than the obtained elements, though the fitting proved satisfying. We decided to provide its elements with significant number comparable to the other satellite for information, but left it without uncertainty.

Satellite	a (km)	e	incl. (EQJ2000)	Ω	ω	v
Himalia	11372100 ± 500	0.166 ± 0.002	45.14 ± 0.15	39.77 ± 0.19	351.48 ± 0.46	97.35 ± 0.48
Elara	11741170 ± 690	0.222 ± 0.002	28.64 ± 0.18	68.42 ± 0.43	179.82 ± 0.56	339.08 ± 0.82
Pasiphae	23425000 ± 5000	0.379 ± 0.001	152.44 ± 0.10	284.59 ± 0.21	135.96 ± 0.19	236.97 ± 0.16
Sinope	22968800 ± 5200	0.316 ± 0.002	157.76 ± 0.12	256.62 ± 0.55	298.38 ± 0.55	167.57 ± 0.19
Lysithea	11739900 ± 1300	0.136 ± 0.004	51.12 ± 0.27	5.53 ± 0.52	53.0 ± 1.5	318.9 ± 2.0
Carme	24202924 ± 4800	0.242 ± 0.001	147.13 ± 0.10	154.01 ± 0.25	47.90 ± 0.29	234.41 ± 0.19
Ananke	21683800 ± 7200	0.380 ± 0.002	172.29 ± 0.20	56.9 ± 1.2	123.3 ± 1.2	231.24 ± 0.21
Leda	11140300 ± 4300	0.173 ± 0.007	16.15 ± 0.75	272.6 ± 1.7	212.2 ± 3.6	218.8 ± 3.2
Themisto	7393800	0.198	25.77	220.0	216.3	262.1

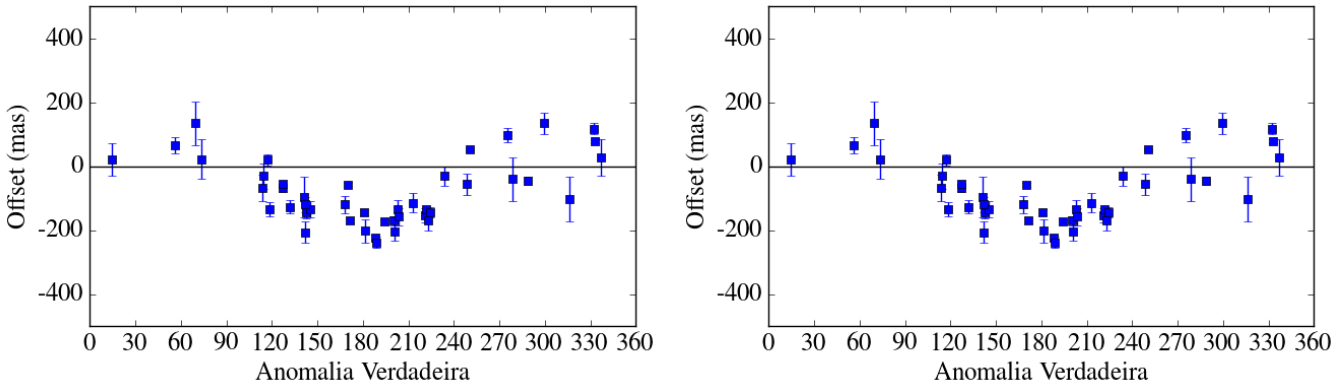

(a) Offset from the JPL ephemeris

(b) Offset from the numerical integration

Fig. 1. Offsets of the declination of Carme by true anomaly from the JPL ephemeris and from the numerical integration of the positions obtained in Gomes-Júnior et al. (2015).

Table 3. Stellar occultation sampled predictions for Himalia I still have to fix the table

d m Year	h m s	RA (ICRS)	Dec	C/A	P/A	v	D	R*	λ	LST	$\Delta e_{\alpha*}$	Δe_{δ}	pm
07 10 2015	21 52 34.	10 53 40.1835	+08 21 00.489	0.465	200.31	39.31	6.25	16.6	179.	09:48	-31.0	-13.0	ok
23 10 2015	07 54 50.	11 05 26.6037	+07 14 32.030	1.017	201.33	36.11	6.12	15.5	16.	08:59	-31.0	-13.0	ok
31 10 2015	00 24 19.	11 10 56.2964	+06 42 07.110	1.801	21.84	33.94	6.04	16.9	123.	08:34	-31.0	-13.0	ok
07 11 2015	21 22 53.	11 16 14.3041	+06 10 05.194	0.306	202.36	31.33	5.94	16.2	162.	08:09	-31.0	-13.0	ok
08 11 2015	04 27 21.	11 16 25.7881	+06 08 55.566	1.077	202.38	31.23	5.94	16.9	55.	08:08	-31.0	-13.0	ok

Notes. Entries included: day of the year and UTC time of the prediction; right ascension and declination of the occulted star - in the original table, these coordinates are immediately followed by the geocentric astrometric equatorial coordinates of the satellite (corrected the computed ephemeris offset derived in Sec. 3); C/A: the geocentric closest approach, in arcseconds; P/A: the planet position angle with respect to the occulted star at C/A, in degrees; velocity in plane of sky, in km s^{-1}: positive = prograde, negative = retrograde; D: planet range to Earth, in AU; R*: normalized magnitude to a common shadow velocity of 20 km s^{-1} by the relationship $\mathrm{Mag}* = \mathrm{Mag}_{\mathrm{actual}} + 2.5 \times \log 10 \left(\frac{\mathrm{velocity}}{20 \mathrm{km\ s^{-1}}} \right)$. A value of 50.0 means that the star is not in the 2MASS; λ: east longitude of subplanet point in degrees, positive towards east; LST: UT + λ: local solar time at subplanet point, hh:mm; $\Delta e_{\alpha*}$ and Δe_{δ}: computed offsets in mas applied to the ephemeris right ascension and declination, respectively; pm: ok = proper motion applied, no = no proper motion applied; catalogue cross-identification (ct) = uc (UCAC2), 2m (2MASS), fs (field star); $E_{\alpha*}$ and E_{δ}: uncertainties (mas) in right ascension and declination. A value of 9999 means that there was no estimation of the respective uncertainty; $\mu_{\alpha*}$ and μ_{δ}: proper motions in right ascension and declination, respectively (mas/year).

For that, we only publish stellar occultations with UCAC4 until 2017.

5. Occultation tests

Observe a stellar occultation demands a great effort. And, in our case, the shadow covers a very restricted area on Earth because the irregular satellites are small. So, before we start a large observational campaign, we tested some occultation predictions for large targets, to assess the quality of the predictions.

The tests consisted in observing the object and star to be occulted near the event when the two objects were present in the same field of view (FOV), preferably when the objects were close to each other. Thus, the relative positions between the two

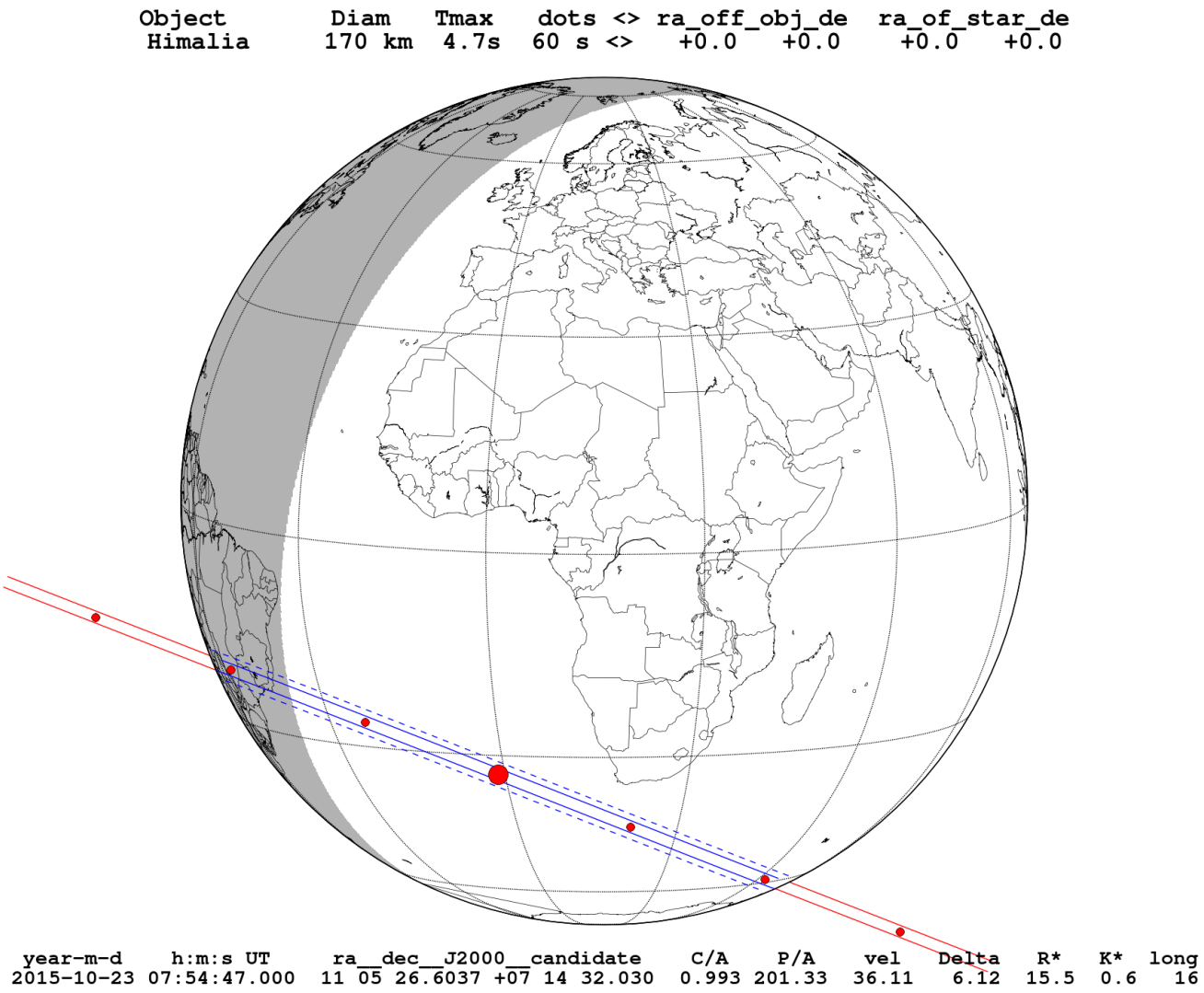

Fig. 2. Occultation map for Himalia regarding to the second event sampled in Table 3

objects had minimal influence of the errors of the reference catalogue of stars used and possible field distortions (Peng et al. 2008, and references therein). The relative positions of the star and of the satellites were used to check the original predictions.

Two occultation tests were performed, one by Himalia that occurred on March 3, 2015 and the second by Elara that occurred on March 30, 2015. For each event, four situations were considered: the first with the nominal positions of the star and the satellite to the predicted time; the second with the offset calculated as described in section 3; the third with star and satellite offsets from observations made a few days before the occultation when the two objects were separated (different FOV); and the fourth from observations made when the star and the satellite were close in the same FOV.

Figure 3shows four zoomed in occultation maps corresponding to each of the four situations for Himalia.. The map 3a is the nominal prediction with the coordinate of the star given by the catalogue and that of the satellite from the ephemeris. We then corrected the positions of the satellite by an offset calculated by the method showed in section 3 to make the map 3b. The map 3c was made from obtained positions on February 22 observed with the Zeiss telescope (diameter = 0.6m; FOV = 12′.6; pixel scale = $0''.37/px$) at the Observatório do Pico dos Dias (OPD, IAU code 874, 45°34′57″W, 22°32′04″S, 1864m). On that day, Himalia and the star were observed in separate FOVs as they were still far apart. On the night of the event, March 3, the objects were observed with Perkin-Elmer telescope (diameter = 1.6m; FOV = 5′.8; pixel scale = $0''.17/px$) at OPD just over an hour after the time scheduled for the event. Satellite and star were separated by about 16 arcsec, so very close to each other. From the calculated offsets, the map 3d was generated. Notice that the shadow path was not predicted to cross the OPD. This was not necessary for testing the prediction.

In this event, it is possible to see that the shade does not vary by much among the four maps suggesting that there was a good probability of observing the event. In fact, the largest differences between the shadows of the four maps were 22s along the shadow path and 109km in the direction perpendicular to the shadows (see table 4).

The second test was with the satellite Elara, which is the second largest irregular satellite of Jupiter. The event was predicted to occur at March 30, 2015. The observations were made

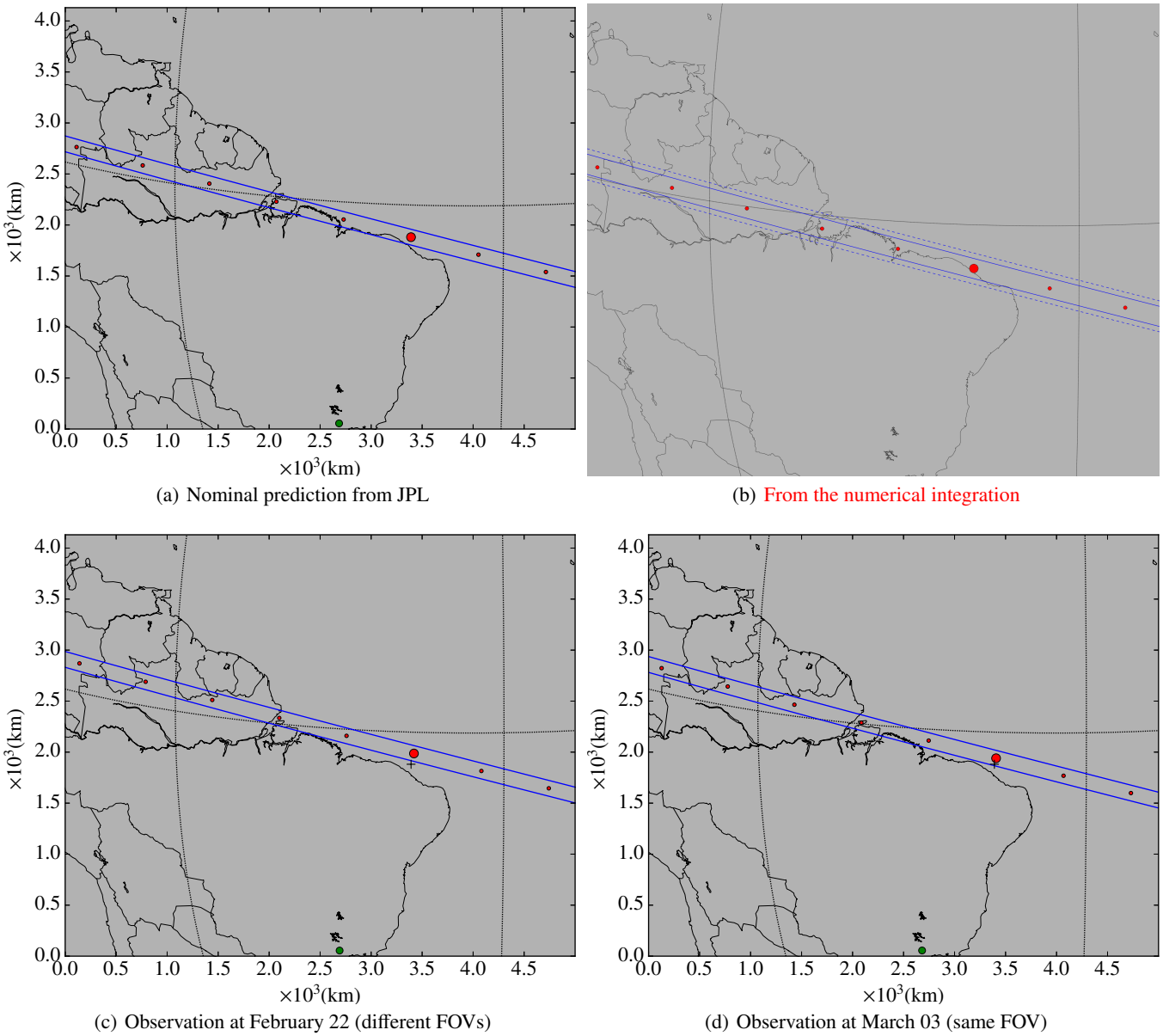

(a) Nominal prediction from JPL

(b) From the numerical integration

(c) Observation at February 22 (different FOVs)

(d) Observation at March 03 (same FOV)

Fig. 3. Predictions for Himalia: The big red dot show the geocentric closest approach of the shadow. The black "+" marks at maps (b,c,d) are the nominal prediction closest approach for reference. The small red ones are the center of the shadow separated by one minute. The straight lines show the size of the shadow. 3a is the map using the nominal positions of the star and satellite. 3b shows the shadow given an estimated offset for the position of Himalia related to the JPL ephemeris obtained in section 3. In 3c we apply offsets to the positions of star and satellite accordingly the observations made at February 22. 3d is as in 3c but with observations made at March 03 when the objects were close to each other. The green dot at the bottom of the maps is the location of Observatório do Pico dos Dias. Figure b waiting for the offset of Himalia

Table 4. Comparison between the predictions of the Himalia occultation at March 03, 2015. Waiting for the right offset

Difference from nominal prediction		
Method	Instant of C/A	C/A
Nominal	00:39:25 UTC	0″.714
Offset		
Feb. 22 Obs.	+12s	-33mas (109km)
Mar. 03 Obs.	-10s	-19mas (61km)

on March 25 and April 2, 2015 with the Zeiss telescope. On the night of April 2 they could still be observed in the same FOV. Due to Elara being fainter than Himalia by 2 magnitudes, dispersions of the satellite positions on both nights ended up being higher than for Himalia. Still, the differences between the maps obtained were relatively small. The largest differences between them were 74s along the shadow path and 307km perpendicular to it (see table 5).

6. Discussion

We presented stellar occultations for the period of 2015-2017 for seven irregular satellites of Jupiter: Ananke, Carme, Elara, Himalia, Lysithea, Pasiphae, and Sinope; one satellite of Saturn: Phoebe; and two satellites of Neptune: Triton and Nereid. The procedure used was the same as that for the prediction of stellar occultations by Pluto and its satellites in Assafin et al. (2010)

Table 5. Comparison between the predictions of Elara occultation at March 30, 2015. Waiting for the right offset

Difference from nominal prediction		
Method	Instant of C/A	C/A
Nominal	01:45:15 UTC	1″.139
Offset		
Mar. 25 Obs.	-59 s	-17mas (61km)
Apr. 02 Obs.	+15 s	-89mas (307km)

Table 6. Number of stellar occultations for each satellite from 2015 up to 2017.

Satellite	2015	2016	2017	Total
Ananke	22	12	16	50
Carme	25	20	14	59
Elara	32	14	16	62
Himalia	25	15	12	52
Lysithea	22	16	11	49
Pasiphae	26	19	20	65
Sinope	19	15	21	55
Phoebe	13	32	98	143
Nereid	41	11	1	53
Triton				

Occultations predicted using the UCAC4 catalogue. For Nereid and Triton, the occultations in 2015 and 2016 were predicted using the WFI catalogue as explained in Sec. 4 Numbers of Triton yet to be written.

and by Centaurs and TNOs in Assafin et al. (2012) and Camargo et al. (2014).

The candidate stars was searched in the UCAC4 catalogue, except for the candidates in 2015 and 2016 for Triton and Nereid. In this case, we used the WFI catalogue that was generated from observations made with ESO2p2/WFI CCD mosaic that covered the path of Neptune in the sky-plane up to 2016 (see Sec. 4).

A total of 588 events were foreseen. In table 6 we present the number of stellar occultations predicted by year for each satellite.

The probability of successfully observing an occultation is roughly the ratio of the satellite's diameter by the budget error of ephemeris and star position. Thus, UCAC4 errors ranging between 20 mas - 50 mas combined with a mean accuracy in the position of 30 mas for Himalia and 100 mas for Ananke mas published in Table 2 of Jacobson et al. (2012) would give 80%-50% probability of observing such an event by Himalia and ≈5% for Ananke, the smallest irregular satellite in the sample. Observations a few days before the date of occultation predicted may improve the combined accuracy to 40-80 mas, depending on the magnitude of the objects.

The tests made with an occultation expected to happen in March 03, 2015 for Himalia showed that this event could probably have been observed in case there were observers available in the shadow area. Fig. 3 shows the maps made for 4 different offset corrections as explained in Sec. 5. Table 4 shows numerically the difference between the maps. A similar test was made for an occultation of Elara in March 30, 2015. The difference between the maps in this case are listed in Table 5.

Continuous observations of the satellites and candidates are recommended and new numerical integrations of the orbits of the satellites are expected to reduce the respective position errors. The GAIA catalogue, which is to be released at the end of 2016 will improve the position error of the stars and will allow for the detection of occultations candidates of fainter stars, which are not present in the UCAC4 catalogue. Consequently, the astrometry of the satellites with the GAIA catalogue will improve the position errors allowing for better predictions and a higher probabilities of observing stellar occultations by irregular satellites.

Acknowledgements. ARG-J thanks the financial support of CAPES. MA thanks the CNPq (Grants 473002/2013-2 and 308721/2011-0) and FAPERJ (Grant E-26/111.488/2013). RV-M thanks grants: CNPq-306885/2013, Capes/Cofecub-2506/2015, Faperj/PAPDRJ-45/2013. JIBC acknowledges CNPq for a PQ2 fellowship (process number 308489/2013-6). FB-R acknowledges PAPDRJ-FAPERJ/CAPES E-43/2013 number 144997, E-26/101.375/2014. BEM thanks the financial support of CAPES.

References

Agnor, C. B. & Hamilton, D. P. 2006, Nature, 441, 192–194
Assafin, M., Camargo, J. I. B., Vieira Martins, R., et al. 2010, Astronomy & Astrophysics, 515, A32
Assafin, M., Camargo, J. I. B., Vieira Martins, R., et al. 2012, Astronomy & Astrophysics, 541, A142
Braga-Ribas, F., Sicardy, B., Ortiz, J. L., et al. 2014, Nature, 508, 72–75
Camargo, J. I. B., Vieira-Martins, R., Assafin, M., et al. 2014, Astronomy & Astrophysics, 561, A37
Clark, R. N., Brown, R. H., Jaumann, R., et al. 2005, Nature, 435, 66–69
de Bruijne, J. H. J. 2012, Astrophysics and Space Science, 341, 31–41
Everhart, E. 1985, in Dynamics of Comets: Their Origin and Evolution, Proceedings of IAU Colloq. 83, held in Rome, Italy, June 11-15, 1984. Edited by Andrea Carusi and Giovanni B. Valsecchi. Dordrecht: Reidel, Astrophysics and Space Science Library. Volume 115, 1985, p.185, ed. A. Carusi & G. B. Valsecchi, 185
Gomes, R., Levison, H. F., Tsiganis, K., & Morbidelli, A. 2005, Nature, 435, 466–469
Gomes-Júnior, A. R., Assafin, M., Vieira-Martins, R., et al. 2015, Astronomy & Astrophysics
Grav, T. & Bauer, J. 2007, Icarus, 191, 267–285
Grav, T., Holman, M. J., Gladman, B. J., & Aksnes, K. 2003, Icarus, 166, 33–45
Jacobson, R., Brozović, M., Gladman, B., et al. 2012, The Astronomical Journal, 144, 132
Jewitt, D. & Haghighipour, N. 2007, Annual Review of Astronomy and Astrophysics, 45, 261–295
Johnson, T. V. & Lunine, J. I. 2005, Nature, 435, 69–71
Lainey, V., Duriez, L., & Vienne, A. 2004, Astronomy and Astrophysics, 420, 1171–1183
McKinnon, W. & Kirk, R. 2007, Encyclopedia of the Solar System, 483–502
Morbidelli, A., Levison, H. F., Tsiganis, K., & Gomes, R. 2005, Nature, 435, 462–465
Nesvorný, D., Alvarellos, J. L. A., Dones, L., & Levison, H. F. 2003, AJ, 126, 398–429
Nesvorný, D., Beaugé, C., & Dones, L. 2004, AJ, 127, 1768–1783
Nesvorný, D., Vokrouhlický, D., & Deienno, R. 2014, ApJ, 784, 22
Nesvorný, D., Vokrouhlický, D., & Morbidelli, A. 2007, AJ, 133, 1962–1976
Ortiz, J. L., Sicardy, B., Braga-Ribas, F., et al. 2012, Nature, 491, 566–569
Peng, Q., Vienne, A., Lainey, V., & Noyelles, B. 2008, Planetary and Space Science, 56, 1807–1811
Porco, C. C., West, R. A., McEwen, A., et al. 2003, Science, 299, 1541–1547
Rettig, T., Walsh, K., & Consolmagno, G. 2001, Icarus, 154, 313–320
Sheppard, S. S. 2005in (Cambridge University Press (CUP)), 319
Sicardy, B., Ortiz, J. L., Assafin, M., et al. 2011, Nature, 478, 493–496
Thomas, P. 2000, Icarus, 148, 587–588
Thomas, P. 2010, Icarus, 208, 395–401
Thomas, P., Veverka, J., & Helfenstein, P. 1991, J. Geophys. Res., 96, 19253
Tsiganis, K., Gomes, R., Morbidelli, A., & Levison, H. F. 2005, Nature, 435, 459–461
Zacharias, N., Finch, C. T., Girard, T. M., et al. 2013, The Astronomical Journal, 145, 44
Ćuk, M. & Burns, J. A. 2004, Icarus, 167, 369–381